

Swift and XMM observations of the dark GRB 050326

A. Moretti^{*}, A. De Luca[†], D. Malesani^{**}, S. Campana^{*}, A. Tiengo[†], J.N. Reeves[‡], M. Capalbi[§], G. Chincarini^{*}, S. Covino^{*}, G. Cusumano[¶], P. Giommi[§], V. La Parola[¶], V. Mangano[¶], T. Mineo[¶], M. Perri[§], P. Romano^{*} and G. Tagliaferri^{*}

^{*}INAF, Osservatorio Astronomico di Brera, via E. Bianchi 46, I-23807 Merate (LC), Italy

[†]INAF, Istituto di Astrofisica Spaziale e Fisica Cosmica di Milano, via E. Bassini 15, I-20133 Milano Italy

^{**}International School for Advanced Studies (SISSA/ISAS), via Beirut 2-4, I-34014 Trieste, Italy

[‡]NASA/Goddard Space Flight Center, Greenbelt Road, Greenbelt, MD20771, USA

[§]ASI Science Data Center, via G. Galilei, I-00044 Frascati (Roma), Italy

[¶]INAF, Istituto di Astrofisica Spaziale e Fisica Cosmica di Palermo, via U. La Malfa 153, I-90146 Palermo, Italy

Abstract. We present a detailed analysis of the GRB 050326 prompt and afterglow emission. The combined capabilities of *Swift* (which sampled the light curve for a relatively long time span) and XMM (which ensured a large statistics) allowed to obtain a thorough characterization of the afterglow properties.

Keywords: gamma rays: bursts – X-rays: individual (GRB 050326)

PACS: 98.70.Rz

GRB 050326 was discovered by the Swift-BAT on 2005 Mar 26 at 9:53:55 UT. Its X-ray coordinates were $\alpha_{J2000} = 00^{\text{h}}27^{\text{m}}49.1^{\text{s}}$, $\delta_{J2000} = -71^{\circ}22'16.3''$, with a 90% uncertainty radius of $1.5''$ containment. This burst was also detected by the *Wind*-Konus experiment, leading to the characterization of its broad-band gamma-ray spectrum (see [1] for the complete description of the observations and the analysis).

The prompt emission was relatively bright (with a 20–150 keV fluence of $\sim 8 \times 10^{-6}$ erg cm⁻²). The spectrum was hard (photon index $\Gamma = 1.25 \pm 0.03$), suggesting a peak energy at the high end of the BAT energy range or beyond. Indeed, thanks to the simultaneous detection of this burst by the *Wind*-Konus experiment [2], the prompt spectrum could be fully characterized. The prompt bolometric fluence was $\mathcal{F} \sim 2.4 \times 10^{-5}$ erg cm⁻² (1–10 000 keV), and the observed peak energy was $E_{\text{p,obs}} = 200 \pm 30$ keV.

Due to pointing constraints, Swift-XRT and Swift-UVOT observations could start only 54 min after the GRB. The X-ray afterglow was quite bright, with a flux of 7×10^{-11} erg cm⁻² s⁻¹ (0.3–8 keV) 1 hr after the GRB. However, no optical counterpart could be detected. The X-ray light curve showed a steady decline, with no breaks or flares. The best-fit power-law decay index was $\alpha = 1.70 \pm 0.05$ (Fig.1). Such regular behaviour is different from that usually observed by *Swift*, but this may be the result of the limited time coverage (observations could be carried out only between 54 min and 4.2 d after the burst). Indeed, extrapolation of the afterglow light curve to the time of the

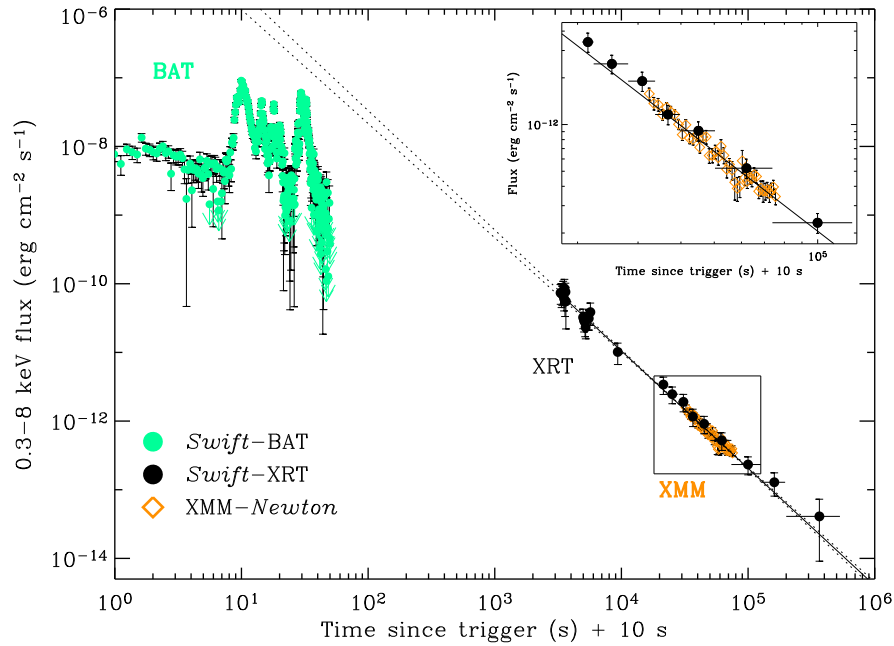


FIGURE 1. The light curve of GRB 050326 and of its afterglow in the 0.3–8 keV energy band. XRT (black circles) and XMM data (empty diamonds) show a very good agreement (see also the inset). The solid line shows the fit to the combined XRT/XMM afterglow light curve. The dotted lines indicate the 90% errors of the extrapolated X-ray light curve. Light filled circles indicate the extrapolation of the BAT data to the 0.3–8 keV energy range, assuming the Band model as the best-fit spectrum. In this figure, the time origin was set 10 s before the nominal trigger time, to show the weak, untriggered precursor. This has no effect on the determination of the afterglow decay slope, due to the late beginning of the XRT observation.

prompt emission overpredicts the burst flux, and may suggest a slower decay before the beginning of the XRT observation.

The analysis of the combined XRT and XMM data allowed to characterize in detail the afterglow spectrum. A fit with an absorbed power-law model provided a good description to the data, yielding a photon index $\Gamma = 2.09 \pm 0.08$ and a column density significantly in excess to the Galactic value. The best-fit model was thus computed adding an extra absorption component, leaving its redshift z free to vary. Although neither $N_{\text{H},z}$ nor z could not be effectively constrained, a firm lower limit $N_{\text{H},z} > 4 \times 10^{21} \text{ cm}^{-2}$ could be set.

Therefore, GRB 050326 adds to the growing set of afterglows with large rest-frame column density [3, 4, 5]. The limits measured in the optical and ultraviolet region by UVOT lie well below the extrapolation of the X-ray spectrum (left panel of Fig 2). In particular, they violate the synchrotron limit that the optical-to-X-ray spectral index should be larger than 0.5. This implies a large extinction and/or a high redshift.

The X-ray spectral analysis also allowed us to set the lower limit $z > 1.5$ to the redshift of the absorbing component and, therefore, of the GRB (right panel of Fig. 2). The isotropic-equivalent gamma-ray energy was then $E_{\gamma,\text{iso}} > 1.4 \times 10^{53} \text{ erg}$. The temporal and spectral properties of the afterglow were nicely consistent with a spherical

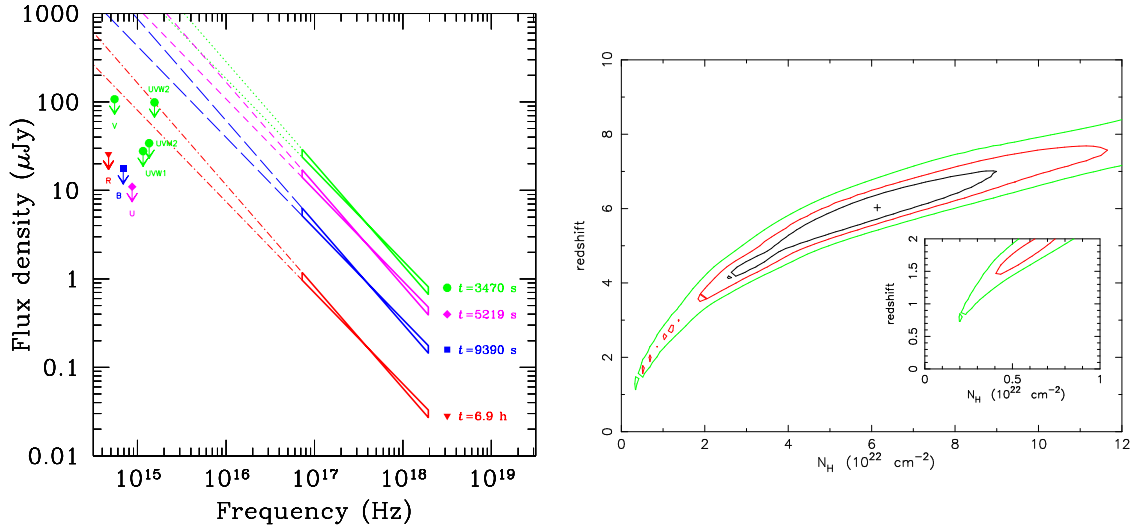


FIGURE 2. **Left Panel.** Broad-band spectral energy distribution of the afterglow of GRB 050326, computed at different times (which are identified by different symbols). The shape of the X-ray spectrum was assumed to be constant throughout the observation, and the decay law was adopted to report the X-ray flux at the time of the optical measurements. **Right Panel.** Confidence contours (68%, 90% and 99% levels for 2 parameters of interest) for the gas column density $N_{H,z}$ and the redshift z of the intrinsic absorber, as computed from the fit to the EPIC spectra. The Galactic column density was assumed to be $N_{H,MW} = 4.6 \times 10^{20} \text{ cm}^{-2}$. The inset shows a zoom-in of the low-redshift region.

fireball expanding in a uniform medium, with the cooling frequency above the X-ray range. We could therefore set a lower limit to the jet break time $t_b > 4 \text{ d}$. The jet opening angle could be constrained to be $\vartheta_j > 7^\circ$, with only a weak dependence on the (unknown) fireball energy. The beaming-corrected gamma-ray energy was $E_{\gamma,j} = (3-8) \times 10^{51} (t_b/4 \text{ d})^{3/4} \text{ erg}$, independently from the redshift. GRB 050326 thus released a large amount of gamma rays (only GRB 990123 had a larger energy in the sample of [6]).

To be consistent with the Ghirlanda relation [6], two redshift ranges are allowed, either at low ($z < 0.8$) or high ($z > 4.5$) redshift (Fig. 3). However, to simultaneously satisfy the limits derived from the X-ray spectral analysis, only the high-redshift region is left. We note that the Ghirlanda relation is still based upon a small sample, so that any inference cannot yet be regarded as conclusive. However, the results from the X-ray spectra, the consistency of the GRB 050326 properties with the Ghirlanda relation, and the strong dearth of optical/ultraviolet afterglow flux, are overall consistent with a moderate/high redshift ($z > 4$). A search for the host galaxy through deep infrared and optical imaging may conclusively settle this issue.

REFERENCES

1. Moretti, A., De Luca, A., Malesani, D., et al. 2006, A&A in press, astro-ph/0512392
2. Golenteskii, S., Aptekar, R., Mazets, E., et al. 2005, GCN Circ. 3152

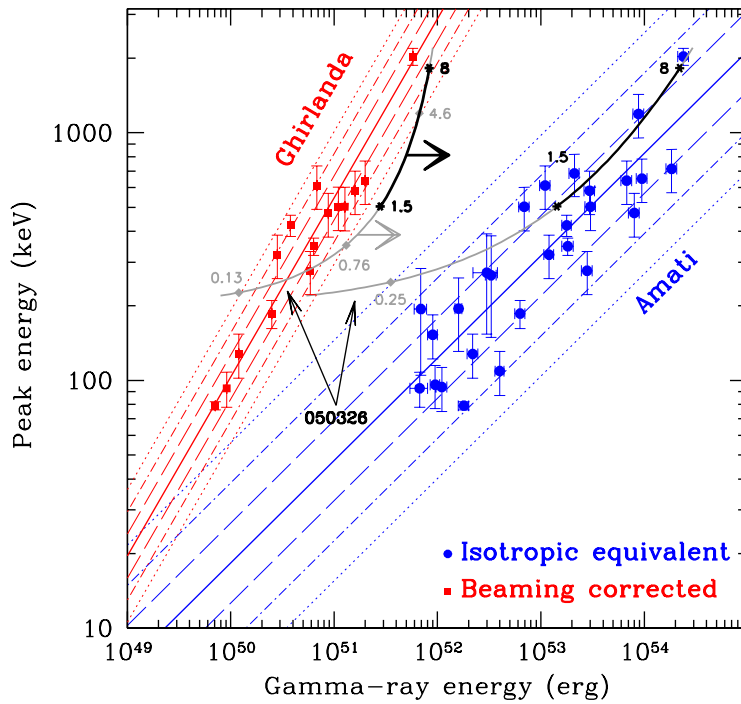


FIGURE 3. Comparison of GRB 050326 with the Amati (right) and Ghirlanda (left) relations [6, 7]. The thick solid curves (black and grey) show the position of GRB 050326 as its redshift varies in the interval $0.1 < z < 10$. The Ghirlanda track is actually a boundary (as the horizontal arrows indicate), since we can only infer a lower limit to the beaming-corrected energy at each redshift. Filled circles and squares indicate the GRBs which define the above two relations, plotted as straight solid lines (together with their 1-, 2- and 3- σ contours: long-dashed, dot-dashed and dotted lines, respectively). Data were taken from [6, 8]. Grey diamonds indicate the intersection of the GRB 050326 tracks with the 3- σ contours of the Amati and Ghirlanda relations. These points thus define the 3- σ redshift ranges for which GRB 050326 was consistent with the two relations. In the two GRB 050326 tracks, the region $1.5 < z < 8$ (indicated by the X-ray data) is shown in black, bound by asterisks.

3. Galama, T.J., & Wijers, R.A.M.J. 2001, *Apj*, 549, L209
4. Stratta, G., Fiore, F., Antonelli, L.A., Piro, L., & De Pasquale, M. 2004, *Apj*, 608, 846
5. Campana, S., Romano, P., Covino, S., et al. 2005b, *A&A*, in press (astro-ph/0511750)
6. Ghirlanda, G., Ghisellini, G., & Lazzati, D. 2004, *Apj*, 616, 331
7. Amati, L., Frontera, F., Tavani, M., et al. 2002, *A&A*, 390, 81
8. Ghirlanda, G., Ghisellini, G., Lazzati, D., & Firmani, C. 2005, *Il nuovo cimento*, in press (astro-ph/0504184)